Environ. Sci. Technol. **2008,** *42,* 5615–5621

Pollutant Emissions from Gasoline Combustion. 1. Dependence on Fuel Structural Functionalities

HONGZHI R. ZHANG,* ERIC G. EDDINGS, AND ADEL F. SAROFIM

Department of Chemical Engineering, The University of Utah, Salt Lake City, Utah 84112

Received October 06, 2007. Revised manuscript received May 19, 2008. Accepted May 19, 2008.

To study the formation of air pollutants and soot precursors (e.g., acetylene, 1,3-butadiene, benzene, and higher aromatics) from aliphatic and aromatic fractions of gasoline fuels, the Utah Surrogate Mechanisms is extended to include submechanisms of gasoline surrogate compounds using a set of mechanism generation techniques. The mechanism yields very good predictions of species concentrations in premixed flames of *n*-heptane, isooctane, benzene, cyclohexane, olefins, oxygenates, and gasoline using a 23-component surrogate formulation. The 1,3-butadiene emission comes mainly from minor fuel fractions of olefins and cyclohexane. The benzene formation potential of gasoline components shows the following trends as functions of (i) chemical class: *n*-paraffins < isoparaffins < olefins < naphthalenes < alkylbenzenes < cycloparaffins < toluene; (ii) carbon number: *n*-butane < *n*-pentane < *n*-hexane; and (iii) branching: *n*-hexane < isohexane < 2,2,4-trimethylpentane < 2,2,3,3-tetramethylbutane. In contrast, fuel structure is not the main factor in determining acetylene formation. Therefore, matching the benzene formation potential of the surrogate fuel to that produced by the real fuel should have priority when selecting candidate surrogate components for combustion simulations.

Introduction

Gasoline is the most important fuel for industrialized societies and accounts for half of the petroleum consumed in the U.S. Emissions from combustion in gasoline engines, therefore, are one of the most serious sources of air pollution (e.g., particulate formation, toxic volatiles, acid rain, and greenhouse gases). Gasoline fuels include paraffinic and aromatic fractions mainly. For example, Hakansson and co-workers (*1*) reported 57.2 and 59.6%, in volume, paraffins in European unleaded certified and California phase-2 reformulated gasoline fuels, respectively. They also reported the aromatic content in the two fuels to be 39.4 and 25.8%, respectively. Huang and co-workers (*2*) reported 24% aromatics and 47% paraffins from C_5 to C_{10} in the Chinese 90# standard unblended gasoline with the peak of the distribution of paraffins being at the hexane and heptane fractions.

For the last several decades, major advances have been made in the ability to predict emissions from the combustion of commercially available fuels (e.g., gasoline) by the use of a surrogate formulation for the fuel and reaction chemistry of individual surrogate components, which usually involves mixtures of paraffins, frequently *n*-heptane and isooctane, since paraffins are the dominant constituents of gasoline and kinetic data are readily available for paraffins. A number of studies have been published concerning the combustion chemistry of paraffinic fractions that are analytically identifiable in gasoline fuels, which includes *n*-heptane (*3–5*), isooctane (*6*), and cyclohexane (*7, 8*). Building on reaction sets of individual surrogate components, gasoline combustion mechanisms were proposed in the literature. Ogink and Golovitchev (*9*) constructed a skeletal gasoline mechanism based on the chemistry of *n*-heptane and isooctane—the two indicator fuels for octane rating. We developed a more detailed Utah Surrogate Mechanisms recently (*10*) that included ~30 submechanisms of surrogate components of paraffins, olefins, and substituted benzenes and naphthalenes. The mechanism yielded successful predictions for a near-stoichiometric premixed flame with a European gasoline (*1*) of conversion rates of major fuel fractions, the distribution of combustion products, and the evolution of major aromatic precursors.

In gasoline combustion mechanisms, olefins are necessary intermediate species formed by the decomposition of paraffins via β-scission and dehydrogenation of alkyl radicals. Olefins also were found to be abundant in one Chinese gasoline fuel (*2*). Studies on olefins include those by Heyberger and co-workers (*11*), who validated a mechanism of butylene with experimental data of a jet-stirred reactor; the study of preautoignition during a rapid compression of 1-pentene (*12*) at low temperatures (600−900 K); and Yahyaoui and co-workers' (*13*) discussion of the ignition of 1-hexene in a shock tube and jet stirred reactor. The general scarcity of olefin chemistry in the literature reflects the current research interests in improving the predictions of paraffinic fuel consumption. To understand environmental impacts from the combustion of fossil fuels and biofuels, confidence in accurate combustion chemistry of olefins should be established. In our earlier studies, we investigated kinetic uncertainties of olefin reactions (*14*) in a few published *n*-heptane mechanisms by comparing the predicted rates of olefin evolution with the measured ones. The major olefin formation reaction classes from alkyl radicals were discussed, in addition to thermal decomposition, radical addition, and other olefin consumption reactions.

Olefin chemistry involves C_3 species (e.g., ally and propargyl radicals), which bridge the paraffin consumption and benzene formation. Two benzene formation classes have been proposed, including (i) propargyl radical combination (*15*) and (ii) acetylene addition (*16*). Formation of aromatics correlates with fuel structural features, as McEnally et al. (*17*) discussed the soot formation trend in doped coflow diffusion methane flame burning heptane isomers. Kaiser and co-workers (*18–20*) at Ford discussed the structural effects on engine-out emissions, including benzene. A more complete list of benzene pathways in terms of fuel structure includes also (iii) the combination of cyclopentadienyl and methyl radicals, (iv) cascading dehydrogenation of cyclohexane moieties, and (v) dealkylation of benzenes. These reaction classes provide the major benzene formation pathways from liquid fuels because of the major presence of ring compounds of aromatics and naphthenes in these fuels (*5, 8, 10*).

Another important environmental concern of combustion includes the formation of acetylene because acetylene is one of the important precursors of soot particle growth (*21*). The chemistry of acetylene in the Utah Surrogate Mechanisms was discussed elsewhere (*22*) and was extensively validated

* Corresponding author phone: (801)349-8680; fax: (801)585-1456; e-mail: westshanghai@yahoo.com.

10.1021/es702536e CCC: $40.75
Published on Web 06/28/2008

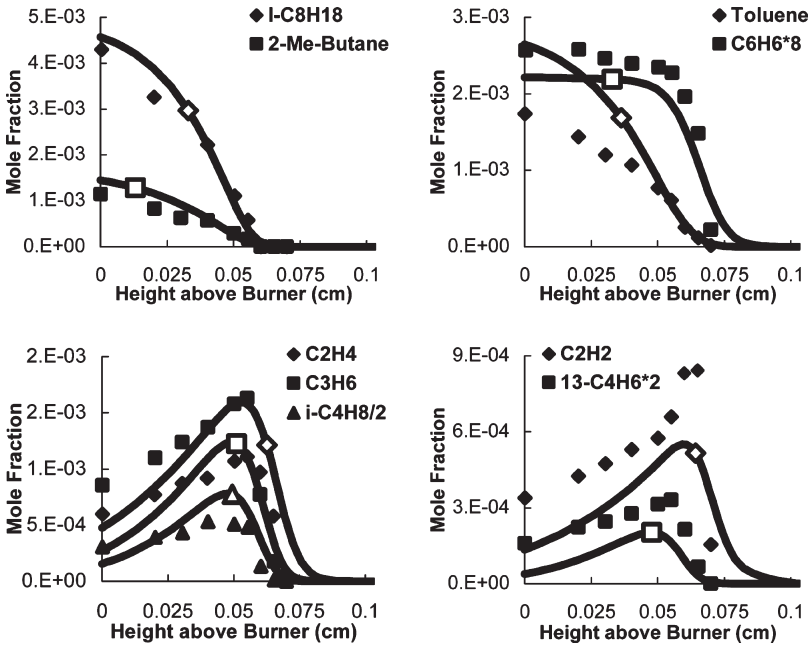

FIGURE 1. Predicted and measured profiles of selected species in the gasoline flame (*1*). The symbols represent the experimental data, and lines with a corresponding symbol are for simulation results.

with experimental data of ~40 flames. Another regulated volatile species is 1,3-butadiene, the formation of which involves the decomposition of cyclohexane (*8, 18*) and olefinic (*19*) fractions in gasoline fuels.

In the current study, the evolution of selected regulated air pollutants and their precursors generated from a premixed gasoline flame is examined critically. The major sources of air pollutants in gasoline fuels are identified. We also focus on correlations between fuel structural functionalities and formation of volatile matter from gasoline combustion in flames and engines, the knowledge of which will provide insights into the pollutant formation potentials of major chemical classes from liquid fuels.

Materials and Methods

The mechanism generation methodology was discussed in a few earlier publications. Generic rates were used extensively to generate selected reaction classes of normal paraffins, and a lumping technique was applied to the decomposition mechanism of methylcyclohexane via the cascading dehydrogenation and ring-opening pathways (*5*). A supplemental technique was used to incorporate a product distribution function into fuel decomposition rate coefficients (*10*), to account for the isomerization reactions among alkyl radicals that are lost during the lumping but very critical for numerical accuracy. The node species technique (*8*) was used in developing a detailed cyclohexane mechanism to curb numerical uncertainties within each pair of consecutive stable intermediate species. These techniques were extensively used during the generation of the Utah Surrogate Mechanisms, in which most submechanisms of gasoline surrogate components (e.g., iso- and cycloparaffins) were generated using combined lumping and product distribution techniques. Most relevant reactions of the mechanism are provided in the Supporting Information (Table S1) for several major gasoline components.

In the current work, a new submechanism of methyl tert-butyl ether (MTBE) was compiled to describe the combustion chemistry of a California gasoline that includes a substantial amount of oxygenates. A few major fuel decomposition reactions of MTBE are added to the Utah Surrogate Mechanisms, and reactions involving combustion intermediates (i.e., isobutylene, methanol, formaldehyde, acealdehyde, propane, and tert-butyl and methoxy radicals) already were included before addition.

The gasoline mechanism will be used to study combustion emissions of gasoline fuels and their individual components, the experimental data of which are taken from the literature. Those experimental data include premixed flames of stabilized burners and engine-out emission studies using a single-cylinder engine. The engine runs on baseline conditions of an equivalence ratio at 0.9, 1500 rpm, and a load of 3.8 bar IMEP (*18*). Details on the experimental information for the seven flames and three engine studies are provided as Supporting Information (Tables S2 and S3).

Models

The Utah Surrogate Mechanisms (*5, 10*) used in the current work was developed for modeling soot and precursor chemistry in pool fires of liquid transportation fuels. The mechanism yielded very good agreements between measured and simulated concentrations of flame intermediates and products. In the current work, a near-stoichiometric (Φ = 0.92) premixed flame measured by Hakansson et al. (*1*) with the California phase-2 reformulated gasoline was simulated using the Utah Surrogate Mechanisms. The simulator used in this study is CHEMKIN IV.

Gasoline fuels usually can be represented by ~20 identifiable compounds or mixtures of isomers. For example, the California phase-2 reformulated gasoline includes 0.3% (by volume) *n*-butane, 7.6% isopentane (IUPAC, 2-methylbutane), ~1.0% *n*-pentane, 11.4% methyl tert-butyl ether, 1.1% *n*-hexane, 1.0% benzene, ~0.5% cyclohexane, 12% toluene, 32.1% isooctane, 6.9% *m*- and *p*-xylene, and 2.2% *o*-xylene. The surrogate used in the current study closely approximates the gasoline fuel including all these compounds that add up to 76.1% of the volume. A lumped species was used to represent all three xylene isomers.

A few fractions were identified to be mixtures of isomers (*1*). For example, the fuel contains 2.8% (by volume) of methylpentanes that are represented by isohexane in this work. Also used in the surrogate formulation was 2,2,3,3-tetramethylbutane to account for a fraction of undistinguishable substituted octane isomers (6.4%). A 6.8% fraction

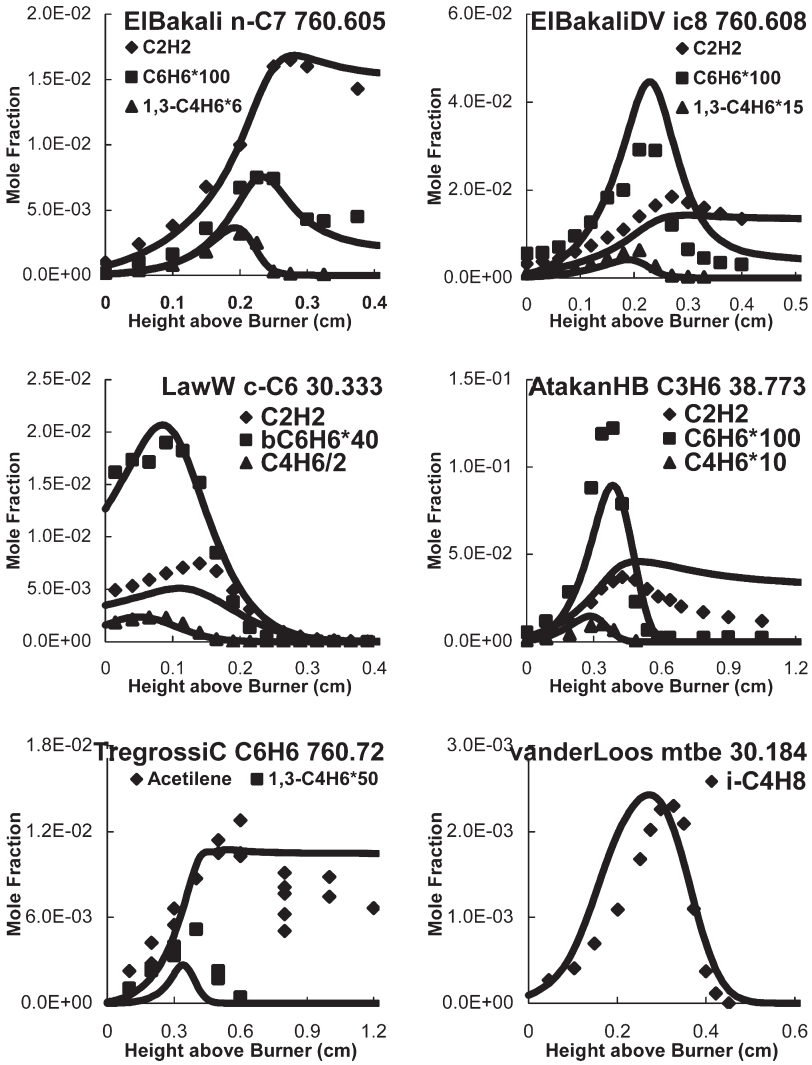

FIGURE 2. Predicted and measured profiles of acetylene, 1,3-butadiene, and benzene in flames of representative fuel components (*4, 7, 24*). The symbols represent experimental data and lines the simulations. The flame designations are combinations of the last name of the first author, initials of other authors, fuel, pressure (torr), and C/O ratio.

was identified to be alkylbenzenes in the experiment likely with C_2-C_5 substituents (*1*). We used a mixture of ethylbenzene (1.0%), ethylmethylbenzene (2.3%), propylbenzene (2.3%), and methylstyrene (1.2%) to represent these unidentifiable aromatic species. Ethylnaphthalene was used as the sole species for the ~0.5% fraction of naphthalenes.

Because olefins in the gasoline fuel were not reported in the flame experiment, we added 5 vol % C_4-C_6 olefins to the surrogate to make the total volume percent unity. The types and distribution of olefins were decided from the data of a recent characterization of the same fuel (*23*), in which olefins from propylene to hexenes were identified. The mixture of olefins in the gasoline surrogate includes 2-butylene (0.43 mol %), isobutylene (0.054 mol %), 2-pentene (2.05 mol %), 1-hexene (0.54 mol %), 2-methyl 2-butene (1.99 mol %), and 2-methyl 1-pentene (1.02 mol %).

Results

The predicted concentrations of selected species of the near-stoichiometric atmospheric premixed flame with the California phase-2 reformulated gasoline are compared with the measured profiles in Figure 1. Hakansson et al. (*1*) characterized the gasoline fuel and reported the four largest fuel fractions, including isooctane (32.1 vol %), toluene (12 vol %), methyl tert-butyl ether (11.4 vol %), and isopentane (7.6 vol %). The authors, however, did not provide the concentration profile of methyl tert-butyl ether. The simulated conversion rates of the major fuel components closely matched the experimental data. The numerical deviations of isopentane and isooctane are particularly small, and the predicted and measured concentrations at locations higher than 0.04 cm from the burner surface show perfect matches. The isopentane and isooctane concentrations at the burner surface were overestimated by 26 and 6%, respectively. The discrepancy is comparable to the experimental uncertainty of the major species, which was estimated to be 25% (*1*). The measured profiles show a clear discontinuity between 0.03 and 0.04 cm above the burner surface, which is more obvious for isopentane. Therefore, flame perturbation during sample extraction can be a major source of numerical deviation near the burner surface. The possible probe effect on the flame structure also is helpful in interpreting the 52% overprediction of toluene at the burner surface because the predicted and measured profiles match each other very well in the later flame zone. The predicted toluene mole fraction at the burner surface is 7% lower than its percentage in the feed, which could be explained by back-diffusion of smaller species. The measured concentration of toluene, however, is 39% lower than the fraction in the feed, which makes it difficult for the simulation to match the experimental value.

Benzene is a minor but regulated component in gasoline fuel. The predicted benzene profile matches the experimental

data quite well with an underprediction of 16% at the burner surface that is progressively narrower at higher locations. The simulation is able to capture the trend in the experimental profile of slow benzene consumption within the reaction zone. Benzene is continuously formed from other fractions in the fuel (e.g., via the cascading dehydrogenation of cyclohexanes (*5, 8, 10, 18*) and dealkylation of substituted benzenes (*18–20*). The consumption of benzene in the feed, therefore, is offset by new formation sources, and the benzene profile exhibits a plateau below 0.06 cm above the burner.

The predicted maximum concentrations of ethylene and propylene are 43% higher and 31% lower than the measured values, respectively. The peak concentration of isobutylene is overpredicted by 48%. The positions of peak concentration are correctly predicted for these olefins. The plateau shape of the measured isobutylene profile between 0.04 and 0.055 cm above the burner surface, however, makes it very difficult for the simulation to capture the experimental trend. A flat region is also visible in the ethylene profile. Flames operated under atmospheric pressure usually introduce major flame perturbation due to probe effects as discussed earlier.

The predicted and measured profiles of two volatile organic compounds are compared in Figure 1. The predicted peak concentrations of acetylene and 1,3-butadiene are underpredicted by 34 and 39%, respectively. The numerical deviations of these species are close to experimental uncertainty.

The reaction submechanisms of major gasoline components were critically examined. Particularly, the chemistry of acetylene, 1,3-butadiene, and benzene was validated in earlier studies for flames of normal and isoparaffins (*5*), naphthenes (*8*), olefins, and aromatics (*22*). The predicted and measured profiles of the fuel and oxygen of selected flames with representative fuels (*4, 7, 24*) are summarized in Figure S1. Those of major volatile organic compounds are compared in Figure 2. It is noted that benzene is the fuel (Figure S1) in the Tregrossi benzene flame and a volatile combustion product in other flames; hydrogen is a fuel in the Van der Loos MTBE flame (Figure S1), in which the profiles of oxygen, acetylene, 1,3-butadiene, and benzene were not measured and a relevant precursor species (isobutylene) was included instead.

The Utah Surrogate Mechanisms yields very good predictions of fuel and oxygen conversion rates for the six flames. The predicted maximum benzene concentration is within or near the reported uncertainty of each flame, with the highest deviations of −27 and +53% seen in the propylene and isooctane flames, respectively. Isoparaffins and olefins, however, are not important sources of benzene (as discussed later). The peak acetylene concentrations are underpredicted by 23 and 32% in isooctane and cyclohexane flames, respectively. The Tregrossi benzene flame has the largest deviation for 1,3-butadiene of −48%. The underprediction, however, will not have significant consequences in gasoline combustion modeling because concentrations of 1,3-butadiene in benzene flames are 2 orders of magnitude lower than those in paraffinic and olefinic flames. In summary, the Utah Surrogate Mechanisms accurately predicts concentrations of major species and critical volatile compounds from the combustion of various fuel classes.

Discussion

To find the major emission sources of volatile matters such as acetylene, 1,3-butadiene, and benzene, which are also critical soot and aromatic precursors, each of the 23 gasoline surrogate components was studied in a modeled flame under the same flame conditions of the gasoline flame (i.e., an equivalence ratio of 0.92, a mass flow rate of 1.2765 g/cm^2 s, a nitrogen content of 76.751 mol % in the feed, and a trace

TABLE 1. Soot Precursor Formation and Emission Pattern of Individual Fuel Components in Atmospheric Premixed Flames (Φ = 0.92); Concentrations in ppm

height above burner	MTBE	*n*-C_4H_{10}	*n*-C_5H_{12}	1-C_6H_{12}	C_6H_6	*n*-C_6H_{14}	$C_6H_5CH_3$	*i*-C_5H_{12}	$C_6H_5C_2H_5$	*i*-C_6H_{14}	$CH_3C_6H_4CH_3$	*i*-C_8H_{18}	$C_6H_5C_3H_7$	C_8H_{18}-2233	$CH_3C_6H_4C_2H_5$	*c*-C_6H_{12}	$C_{10}H_7C_2H_5$	*i*-C_4H_8	2-C_4H_8	2-C_5H_{10}
composition (mol %)	12.93	0.38	1.19	0.54	1.51	1.13	15.36	8.89	1.13	2.91	10.08	26.24	2.26	5.33	2.26	0.65	0.43	0.05	0.43	2.05
benzene at 0.033 cm	0.352	0.0787	0.263	2.28	14900	0.353	315	0.502	40.5	0.66	18.5	0.877	78.2	1.18	26.4	264	9.24	2.29	32.5	3.80
benzene at 0.0511 cm	0.599	0.117	0.377	3.25	6750	0.493	571	0.822	93.3	1.09	35.5	1.59	152	2.14	54.9	446	20.2	4.16	64.8	6.62
benzene at 0.0659 cm	0.259	0.0291	0.0779	0.62	1200	0.0953	546	0.268	90.2	0.32	47	0.973	135	1.40	89.4	105	37.2	3.17	105	2.45
acetylene at 0.061 cm	420	469	491	552	399	498	345	556	279	568	284	596	367	603	383	511	232	598	569	573
butadiene at 0.0495 cm	15.8	11.1	82.8	606	6.78	108	3.37	156	2.35	177	0.662	27.3	3.98	28.1	1.38	1430	0.32	32.6	1.37	1130
aromatic at 0.0511 cm	2.16	0.431	1.51	15.2	11400	2.02	12250	3.50	8390	4.67	9520	6.04	5140	7.93	9430	777	8845	15.2	10700	35.5

height above burner	2-me-2-C_4H_8	2-me-1-C_5H_{10}	$CH_3C_6H_4C_2H_3$	full surrogate
composition(mol %)	1.99	1.02	1.24	
benzene at 0.033 cm	4.33	4.22	32.5	274
benzene at 0.0511 cm	8.09	7.55	64.8	253
benzene at 0.0659 cm	5.38	3.03	105	128
acetylene at 0.061 cm	583	612	569	550
butadiene at 0.0495 cm	695	424	1.37	101
aromatic at 0.0511 cm	49.6	43.5	10700	3140

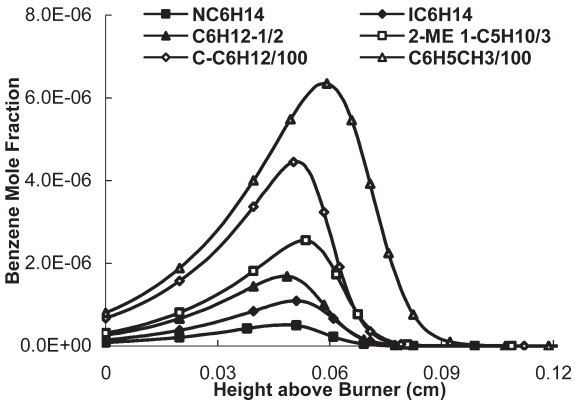

FIGURE 3. Predicted benzene concentrations in modeled flames with C_6 gasoline components (*n*-, iso-, and cyclohexanes, 1-hexene, and 3-methyl 1-pentene) and toluene. The benzene formation potential follows the order *n*-paraffins < isoparaffins < straight olefins < substituted olefins ≪ cycloparaffins < aromatics.

amount of krypton (0.991%)). Also, the temperature profile of the gasoline flame was used for the 23 modeled flames of individual compounds, and the temperature reached a maximum of 2000 K at 0.1055 cm above the burner. The predicted concentrations of benzene at three locations and acetylene, 1,3-butadiene, and C_5+ aromatics at one location each are reported in Table 1. The predicted benzene concentration in the gasoline flame using the full surrogate is initially close to constant and then declines sharply at locations higher than 0.06 cm (Figure 1). Therefore, the chosen locations correspond to three different regions of the benzene profile in the gasoline flame.

Chemical Class Dependence. The benzene formation potential highly correlates with structural functionalities of chemical classes. The most important benzene sources among surrogate components in Table 1 include the cascading dehydrogenation of cyclohexane (*8*) producing 446 ppm at 0.0511 cm above the burner surface and the dealkylation of toluene yielding 571 ppm, in addition to the benzene fraction in the feed. Components of other chemical classes produce much less benzene. For engines, benzene formation can be greatly enhanced by dealkylation of substituted benzenes by certain catalysts (*25*). The benzene formation potential at 0.0511 cm above the burner surface follows the order of normal paraffins and MTBE (a fraction of parts per million) < isoparaffins (1−2 ppm) < straight olefins (3−6 ppm) < substituted olefins (4−8 ppm) ≪ ethylnaphthalene (20 ppm) ≪ alkylbenzenes (40−150 ppm) ≪ cyclohexane and toluene (450 and 570 ppm), in comparison to 253 ppm obtained in the gasoline flame. The value is close to those of single-ring cyclics in the fuel. The order is illustrated in Figure 3 of the benzene formation potential from toluene and C_6 species. The oxygenated MTBE produces <1 ppm benzene, which is comparable to that from paraffins.

Single fuels were studied at a fixed equivalence ratio of 0.9 under the same engine conditions in earlier Ford experiments of engine-out emission (*18*–*20*) from crevices within the cylinder and in the exhaust system. The emission data compiled from those studies are presented in Table 2. The order of benzene emission matches that found in flames as *n*-paraffins (not visible) < isoparaffins and straight olefins (0−6 ppm) < substituted olefin diisobutylene (11 ppm) < xylenes and ethylbenzene mixture (48 ppm) < naphthalenes (54−60 ppm) < toluene (95 ppm). The fully blended gasoline yielded 55 ppm benzene, which matched those of cyclics. This correspondence has important ramifications concerning the mechanisms for engine-out emissions. The good agreement of the trends in emissions of regulated species in engines and trends in flames implies that these emissions are flame-generated combustion products.

A very similar dependence on chemical classes was observed for the formation potential of C_5+ aromatics in modeled component flames and in the engine-out emission experiments as well. The flame results show the order of normal paraffins and MTBE (1−2 ppm) < isoparaffins (3−8 ppm) < straight olefins (15−35 ppm) < substituted olefins (15−50 ppm) ≪ cyclohexane (777 ppm) ≪ alkylbenzenes and naphthalenes (5000−10500 ppm) < benzene and toluene (about 12000 ppm). In contrast, the formation of acetylene in flames and engine experiments does not depend on the fuel chemical classes. Engine-emitted acetylene is due to the persistence of acetylene in the postflame gases, which is different from the outgassing of fuel combustion products in crevices. In flames, olefins yield the largest amount of acetylene with the highest concentration of 612 ppm produced by 2-methyl 1-pentene. Ethylnaphthalene yields the lowest level of acetylene at 232 ppm, followed by ethylbenzene and xylene at ∼280 ppm. The order of acetylene formation potential is naphthalenes (230 ppm) < benzenes (280−400 ppm) < MTBE and normal and cycloparaffins (420−500 ppm) < isoparaffins and olefins (550−600 ppm). The energy barrier of the ring opening is probably responsible for the lower acetylene concentration from aromatic compounds in flames. Nonaromatic compounds, including cyclic naphthenes, produce almost similar amounts of acetylene.

The formation potential of 1,3-butadiene varies significantly among different fuel chemical classes with naphthenes yielding the highest 1,3-butadiene concentration at 1430 ppm in flames (Table 1) and 120−135 ppm in engine-out emissions (Table 2). The principal butadiene formation route from cyclohexane was proposed (*8*) to be the ring opening pathway followed by isomerization from 1-hexen-6-yl to 1-hexen-3-yl radicals via an internal 1−4 hydrogen migration. In general, 1,3-butadiene is a major combustion intermediate from fuel fractions with a hydrogen deficiency of 1 (e.g., cyclohexanes and olefins). Olefins yield high levels of 1,3-butadiene at 400−1100 ppm in flames and 62−94 ppm emitted from the engine. In contrast, aromatic fuels yield a very low concentration of 1,3-butadiene in both systems, and normal and isoparaffins produce moderate amounts of 1,3-butadiene.

Carbon Number Dependence. The benzene formation potential also correlates with the length of the carbon chain (carbon number) within a chemical class as demonstrated in Figure 4. For example, the predicted benzene concentrations at 0.0511 cm above the burner surface of normal butane, pentane, and hexane are 0.1, 0.4, and 0.5 ppm, respectively. A similar trend of homologous isoparaffins also is seen in Figure 4 (i.e., isopentane yielding less benzene than isohexane). The same pattern is observed in Table 1 and Figure 4 for other chemical classes (e.g., 2-butylene and 2-pentene, isobutylene and 2-methyl 1-pentene, ethyl- and propylbenzenes, and xylene and ethylmethylbenzene) and in engine studies for 1-butene and 1-hexene.

The concentrations of 1,3-butadiene in modeled component flames and engine studies demonstrate a strong dependence on the carbon number and follow the exact same orders as what were observed for benzene formation. The total concentration of C_5+ aromatics increases with the carbon number of olefins and all types of paraffins in flame and engine studies. However, the longer substituents in ethylmethyl- and propylbenzenes do not lead to higher aromatic concentrations than in xylenes and ethylbenzene, respectively, probably because the aliphatic chains reduce the percentage of aromatic carbons.

In contrast, the higher homologous propylbenzene in Table 1 produces 367 ppm acetylene, ∼100 ppm more than that from ethylbenzene (279 ppm). The longer aliphatic chains promote the formation of acetylene in contrast to the

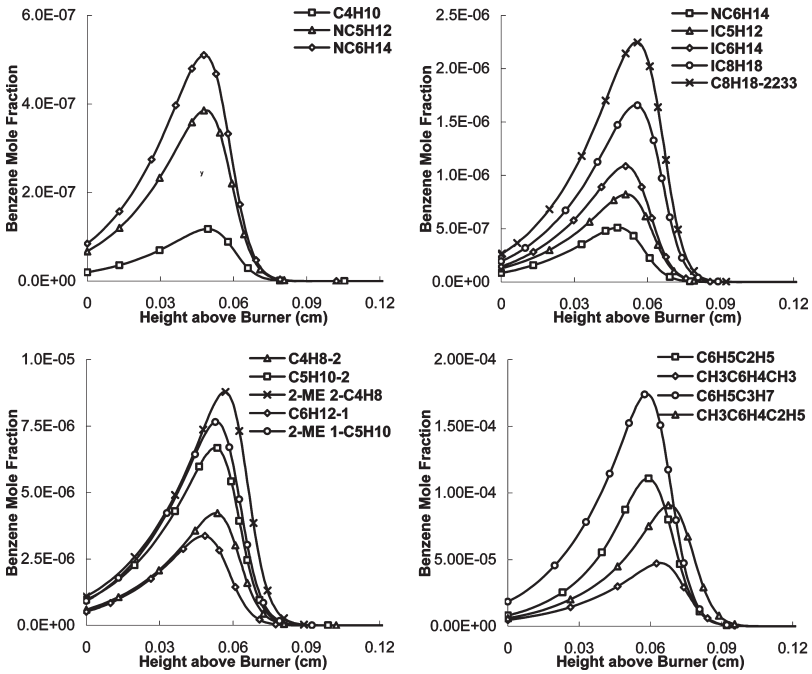

FIGURE 4. Predicted benzene concentrations in modeled normal and isoparaffin, olefinic, and aromatic flames. The fuels with a higher carbon number produce more benzene following the order *n*-butane < *n*-pentane < *n*-hexane and isopentane < isohexane. The fuels with higher branching factors produce more benzene (e.g., *n*-hexane < isohexane < isooctane < 2,2,3,3-tetramethylbutane), and the straight olefins yield less benzene than substituted olefins with the same carbon number. The terminal olefins produce less benzene than internal olefins. In contrast, the higher substituted aromatic fuels produce less benzene as the formation potential follows the order dimethylbenzene < ethylbenzene and methylethylbenzene < propylbenzene.

TABLE 2. Measured Species Concentrations in Exhaust for Single Fuels and Fuel Blends with Equivalence Ratio Fixed at 0.9[a]

fuel	*n*-C_4H_{10}	*i*-C_5H_{12}	*i*-C_8H_{18}	*c*-C_6H_{12}	*c*-$C_6H_{11}CH_3$	1-C_4H_8	1-C_6H_{12}
acetylene	29 ppm C	49	38	60	53	39	48
1,3-butadiene	7	13	8	135	120	62	94
benzene	not visible	not visible	6	54	60	not visible	6
aromatics[b]	not visible	not visible	6	54	72	not visible	6

fuel	diisobutene	$C_6H_5CH_3$	*n*-C_6H_{14} + $C_6H_5CH_3$	$CH_3C_6H_4CH_3$ + $C_6H_5C_2H_5$	tracer	gasoline	diisobutene + gasoline
acetylene	40	54	46	40	44	44	35
1,3-butadiene	10	7	18	5	10	28	22
benzene	11	95	47	48	43	55	37
aromatics	11	1816	619	1741	547	365	254

[a] Compiled from refs *18–20*. [b] Aromatic concentration includes those of detected species in engine emission.

weaker acetylene production from the ring opening of aromatics as discussed earlier in terms of chemical class dependence. In general, there is only a weak dependence of acetylene formation in flames on the carbon number of paraffins and olefins because the deviation of acetylene concentrations is usually within 5% of the arithmetic mean of each class.

Branching Factor Dependence. A correlation is identified in the current work between the branching factor and the formation of benzene and other aromatics, which are soot precursors. In Figure 4, the maximum benzene concentrations from paraffinic fuels follow the order of normal hexane (0.5 ppm) < isohexane (1.1 ppm) < isooctane (1.6 ppm) < 2,2,3,3-tetramethylbutane (2.1 ppm). The branching effect on the benzene formation also is observed in Figure 4 between 2-pentene and 2-methyl 2-butylene and 1-hexene and 2-methyl 1-pentene. Multiple substituents on the benzene ring (e.g., ethylmethylbenzene versus propylbenzene), however, do not translate into higher benzene concentrations because more dealkylation steps are needed to produce benzene.

In contrast, the yield of C_5+ aromatics from benzenes increases with the number of substitutions as seen in Table 1, probably because benzylic radicals obtained by the hydrogen abstraction of aliphatic substituents facilitate the formation of higher aromatic compounds (*22*). In general, the concentrations of C_5+ aromatic species with other fuel classes depend on the branching factor following the trends of benzene concentrations.

The branching effect on 1,3-butadiene formation involves the shape of the carbon flame of fuel molecules. For example, isopentane produces more 1,3-butadiene (156 ppm at 0.0495 cm above the burner surface) than *n*-pentane (82.8 ppm) due to the lower energy barriers of possible routes via demethylation and internal olefins. In contrast, the octanes and their conjugate olefins in Tables 1 and 2 yield much less 1,3-butadiene because decomposition of these species leads to mainly iso-C_4 moieties, which effectively inhibit the formation of 1,3-butadiene. The lower 1,3-butadiene concentrations from isobutylene, 2-methyl 2-butylene, 2-methyl 1-pentene, and disubstituted benzenes in comparison to their isomers provide additional evidence of the importance in

matching the shape of major fuel decomposition fragments with the structure of 1,3-butadiene.

Benzene Formation Pathways. The correlations between benzene concentrations and fuel functionalities call for further studies of major benzene formation pathways. The pathways of C_2H_2 addition (*16*) and the combination of C_3 species (*15*) have been well-studied. The cascading dehydrogenation of cyclohexanes and dealkylation of substituted benzenes are relatively new to combustion modeling. Benzene emission during combustion of liquid transportation fuels, however, comes mainly from naphthene and aromatic fuel fractions. Those benzene formation pathways need to be fully tested under various combustion conditions.

A very important conclusion can be made for the relative importance of major benzene formation pathways with paraffinic fuels. The correlation between the 1,3-butadiene formation and the branching factor breaks down for certain isoparaffinic fuels (e.g., octanes). In an earlier study (*5*), the experimental premixed flame data of normal heptane and isooctane under fuel-rich conditions were simulated. The measured peak concentrations of acetylene (16 000 ppm in the C_7 flame/18 00 ppm in the C_8 flame) and 1,3-butadiene (530:420) in these two flames are comparable to each other. The predicted concentrations were within 20% of the experimental data with the exception of the underprediction of 1,3-butadiene in the isooctane flame by 35%. Under near-stoichiometric conditions, a more significant reduction of 1,3-butadiene in octane flames is observed in Table 1. Therefore, in octane flames, 1,3-butadiene formation does not increase with the branching factor, while benzene concentrations strongly correlate with the branching factor. Because the chemistry of 1,3-butadiene significantly affects concentrations of other C_4 species (*22*), pathways involving C_4 species alone are not adequate to reproduce the pattern of benzene concentrations in flames of octane fuels.

Acknowledgments

This research was funded by the University of Utah (C-SAFE), through a contract with the Department of Energy, Lawrence Livermore National Laboratory (B341493).

Supporting Information Available

This material (reaction kinetics, experimental settings, and mechanism validation information) is available free of charge via the Internet at http://pubs.acs.org.

Literature Cited

(1) Hakansson, A.; Stromberg, K.; Pedersen, J.; Olsson, J. O. Combustion of gasolines in premixed laminar flames. European certified and California phase 2 reformulated gasoline. *Chemosphere* **2001**, *44*, 1243.
(2) Huang, C.; Wei, L.; Yang, B.; Wang, J.; Li, Y.; Sheng, L.; Zhang, Y.; Qi, F. Lean premixed gasoline/oxygen flame studied with tunable synchrotron vacuum UV photoionization. *Energy Fuels* **2006**, *20*, 1505.
(3) Curran, H. J.; Gaffuri, P.; Pitz, W. J.; Westbrook, C. K. A comprehensive modeling study of *n*-heptane oxidation. *Combust. Flame* **1998**, *114*, 149.
(4) El Bakali, A.; Delfau, J. L.; Vovelle, C. Experimental study of 1 atm, rich, premixed *n*-heptane and isooctane flames. *Combust. Sci. Technol.* **1998**, *140*, 69.
(5) Zhang, H. R.; Eddings, E. G.; Sarofim, A. F. Combustion reactions of paraffin components in liquid transportation fuels using generic rates. *Combust. Sci. Technol.* **2007**, *179*, 61.
(6) Pitsch, H.; Peters, N.; Seshadri, K. Numerical and asymptotic studies of the structure of premixed isooctane flames. *Proc. Combust. Inst.* **1996**, *26*, 763.
(7) Law, M. E.; Westmoreland, P. R.; Cool, T. A.; Wang, J.; Hansen, N.; Kasper, T. Benzene precursors and formation routes in a stoichiometric cyclohexane flame. *Proc. Combust. Inst.* **2007**, *31*, 565.
(8) Zhang, H. R.; Huynh, L. K.; Kungwan, N.; Yang, Z.; Zhang, S. Combustion modeling and kinetic rate calculations for a stoichiometric cyclohexane flame. Part I. Major reaction pathways. *J. Phys. Chem. A* **2007**, *111*, 4102.
(9) Ogink, R.; Golovitchev, V. Gasoline HCCI modeling: Computer program combining detailed chemistry and gas exchange processes. *Soc. Automot. Eng., [Spec. Publ.] SP-1642* **2001**, 93.
(10) Zhang, H. R.; Eddings, E. G.; Sarofim, A. F. Criteria for selection of components for surrogate of natural gas and transportation fuels. *Proc. Combust. Inst.* **2007**, *31*, 401.
(11) Heyberger, B.; Belmekki, N.; Conraud, V.; Glaude, P. A.; Fournet, R.; Battin-Leclerc, F. Oxidation of small alkenes at high temperatures. *Int. J. Kinetics* **2002**, *34*, 666.
(12) Minetti, R.; Roubaud, A.; Therssen, E.; Ribaucour, M.; Sochet, L. R. The chemistry of pre-ignition of *n*-pentane and 1-pentene. *Combust. Flame* **1999**, *118*, 213.
(13) Yahyaoui, M.; Djebaili-Chaumeix, N.; Paillard, C. E.; Touchard, S.; Fournet, R.; Glaude, P. A.; Battin-Leclerc, F. Experimental and modeling study of 1-hexene oxidation behind reflected shock waves. *Proc. Combust. Inst.* **2005**, *30*, 1137.
(14) Zhang, H. R.; Eddings, E. G.; Sarofim, A. F. Olefin chemistry in a premixed heptane flame. *Energy Fuels* **2007**, *21*, 677.
(15) Miller, J. A.; Melius, C. F. Kinetic and thermodynamic issues in the formation of aromatic compounds in flames of aliphatic fuels. *Combust. Flame* **1992**, *91*, 21.
(16) Frenklach, M.; Warnatz, J. Detailed modeling of PAH profiles in a sooting low-pressure acetylene flame. *Combust. Sci. Technol.* **1987**, *51*, 265.
(17) McEnally, C. S.; Ciuparu, D. M.; Pfefferle, L. D. Experimental study of fuel decomposition and hydrocarbon growth processes for practical fuel components: Heptanes. *Combust. Flame* **2003**, *134*, 339.
(18) Kaiser, E. W.; Siegl, W. O.; Cotton, D. F.; Anderson, R. W. Effect of fuel structure on emissions from a spark-ignited engine. 2. Naphthene and aromatic fuels. *Environ. Sci. Technol.* **1992**, *26*, 1581.
(19) Kaiser, E. W.; Siegl, W. O.; Cotton, D. F.; Anderson, R. W. Effect of fuel structure on emissions from a spark-ignited engine. 3. Olefinic fuels. *Environ. Sci. Technol.* **1993**, *27*, 1440.
(20) Kaiser, E. W.; Siegl, W. O.; Henig, Y. I.; Anderson, R. W.; Trinker, F. H. Effect of fuel structure on emissions from a spark-ignited engine. *Environ. Sci. Technol.* **1991**, *25*, 2005.
(21) Frenklach, M.; Wang, H. Detailed mechanism and modeling of soot particle formation. In *Soot Formation in Combustion: Mechanisms and Models*; Bockhorn, H., Ed.; Springer-Verlag: Berlin, 1994; pp 165−192..
(22) Zhang, H. Numerical Combustion of Commercial Fuels and Soot Formation. Ph.D. Thesis, University of Utah, Salt Lake City, UT, 2005.
(23) Schauer, J. J.; Kleeman, M. J.; Cass, G. R.; Simoneit, B. R. Measurement of emissions from air pollution sources. 5. C_1−C_{32} organic compounds from gasoline-powered motor vehicles. *Environ. Sci. Technol.* **2002**, *36*, 1169.
(24) (a) Atakan, B.; Hartlieb, A. T.; Brand, J.; Kohse-Hoinghaus, K. An experimental investigation of premixed fuel-rich low-pressure propene/oxygen/argon flames by laser spectroscopy and molecular-beam mass spectrometry. *Proc. Combust. Inst.* **1998**, *27*, 435. (b) Tregrossi, A.; Ciajolo, A.; Barbella, R. The combustion of benzene in rich premixed flames at atmospheric pressure. *Combust. Flame* **1999**, *117*, 553. (c) Van Der Loos, A.; Vandooren-Van, J.; Tiggelen, P. J. Kinetic study of methyl tert-butyl ether (MTBE) oxidation in flames. *Proc. Combust. Inst.* **1998**, *27*, 477.
(25) Bruehlmann, S.; Forss, A. M.; Steffen, D.; Heeb, N. V. Benzene: A secondary pollutant formed in the three-way catalyst. *Environ. Sci. Technol.* **2005**, *39*, 331.

ES702536E